Metataxonomic signature of beef burger perishability depends on the meat origin prior grinding

Metataxonomic signature of beef burger perishability depends on the meat origin prior grinding

Cristian Botta, Irene Franciosa, Valentina Alessandria, Vladimiro Cardenia, Luca Cocolin, Ilario Ferrocino*.

Department of Forestry, Agriculture and Food Sciences, University of Torino, Italy.

Running title: Potentiality of metataxonomic analysis to detect batch variability

Key words: ground beef, metataxonomic, metabolomic, spoilage profiles

* Corresponding author:
Department of Agricultural, Forest, and Food Science, University of Turin, Largo Paolo Braccini 2, 10095, Grugliasco, Torino, Italy. E-mail address: ilario.ferrocino@unito.it (IF)

Abstract

Spoilage dynamics of two hamburger batches from different beef origins were followed from their shared processing run until the use-by date and beyond. Amplicon based sequencing of bacterial and fungal communities were compared with microbial counts and volatilome profile in order to determine whether and at which extent their perishability was related to the batch origin.

Microbiological counts did not differ between batch A and B, whereas Volatile Organic Compounds (VOCs) profiles were only distinguishable after the use-by date. Metataxonomic analysis showed that both batches shared the same initial fungal and bacterial community, which however represented a transient signature of the processing run. Indeed, it was rapidly replaced by batch-autochthonous species

of fungi and bacteria. Different temporal succession patterns of psychotropic lactic acid bacteria (LAB) were observed between the batches from the fourth day of vacuum storage. In particular, the sequential dominance of *Carnobacterium divergens* and *Leuconostoc piscium* in batch B was correlated with a more heterogeneous volatilome and greater production of VOCs linked to off-odours, such as the acetoin. The metataxonomic survey was able to discriminate between the two batches of hamburgers in relation to their origin and regardless of the initially shared processing-derived contamination.

1.INTRODUCTION

Meat consumption has increased worldwide in the last decades in relation to the greater demand from developing countries, in which the growing economic prosperity shifted the dietary habits towards a larger consumption of animal derived proteins (Bonnet, Bouamra-Mechemache, Réquillart, & Treich, 2020). It is therefore a concern that every year great percentages of meat products are wasted due to premature spoilage caused by bacteria, molds and yeasts development (Luong, Coroller, Zagorec, Membré, & Guillou, 2020). Indeed, shelf life depends to the tight relationship between physical-chemical composition of a given product and its microbiota. Food organoleptic traits are associated with the metabolic activities of beneficial or unwanted microbial communities, which alternatively determine shelf-life prolongation or reduction (De Filippis, Parente, & Ercolini, 2018).

High physical-chemical heterogeneity between different batches characterises meat and influences its initial microbial diversity (Pieszczek, Czarnik-Matusewicz, & Daszykowski, 2018). The initial composition of this animal-derived microbiota is subsequently modified by environmental sources of contamination, such as the operator's handling, water, air and the contact with equipment surfaces (Botta, Ferrocino, Pessione, Cocolin, & Rantsiou, 2020; Chaillou et al., 2015; Stellato et al., 2016). Impact of process-derived contamination on the final shelf life are particularly high when hygienic parameters suggested by the Good Manufacturing Practices (GMPs) are not fully accomplished (de Filippis, La

Storia, Villani, & Ercolini, 2013; Redondo-Solano et al., 2021). After packaging, the gaseous atmosphere and the maintenance of the cold-supply chain are the only means available to contrast a premature spoilage by slowing down microbial growth.

Among fresh meat products, beef burger is more prone to pigment degradation, proteins denaturation and lipid oxidation than intact muscle cuts. The increased surface area leads to high nutrients availability for the microbes growth and favors their catabolic activities (Bao, Puolanne, & Ertbjerg, 2016; Limbo, Torri, Sinelli, Franzetti, & Casiraghi, 2010). In relation to the ISO standards for the enumeration of spoilage population in meat its shelf-life under vacuum packages (VP) spans from ten to fourteen days (Pothakos, Snauwaert, De Vos, Huys, & Devlieghere, 2014). However, the number of biochemical reactions rises considerably in parallel to the microbial growth and compounds related to undesirable sensory changes are produced even before the use-by date (Hultman, Johansson, & Björkroth, 2020; Pothakos, Devlieghere, Villani, Björkroth, & Ercolini, 2015; Valerio et al., 2020).

One of the major causes of off-flavours and off-odours in ground beef is the lipid oxidation with the following formation of Volatile Organic Compounds (VOCs) like aldehydes and ketones (Valerio et al., 2020). Overall, VOCs accumulation over certain thresholds can lead to products rejection due to rancidity odours and meat colour change (Casaburi, Piombino, Nychas, Villani, & Ercolini, 2015). These compounds come from the enzymatic degradation of amino acids, of which psychotrophic LAB, *Brochothrix thermosphacta* and *Pseudomonas* spp. are known to be the main responsible (Casaburi et al., 2015; Pennacchia, Ercolini, & Villani, 2011). Conversely, little is known on yeasts and molds involvement in the spoilage of chilled packaged meat during shelf-life (Yang, Che, Qi, Liang, & Song, 2017), while in dry cold-aged beef the mycobiota is known to alternatively play a spoilage and pro-technological role in relation to the species developed on the crust (Mikami et al., 2021; Oh, Lee, Lee, Jo, & Yoon, 2019; Ryu et al., 2018).

In this context, meat industries are constantly seeking for preventative techniques able to maximize the shelf-life of ground beef products by reducing or limiting their initial contamination levels. Different possible strategies have been proposed to accomplish this request: boosting the in-house sanitizing methods with environmental ozone treatments (Botta et al., 2020), prior-grinding decontamination of meat cuts with electrolyzed water (Botta et al., 2021, 2018), and the use of biopreservatives during shelf-life (Ferrocino, Greppi, Lastoria, Rantsiou, & Ercolini, 2016; Grispoldi, Karama, Sechi, Iulieto, & Cenci-Goga, 2020). It was however noticed that any preventative technique can be more or less effective in relation to the initial microbiota composition of the treated product, which varies between production runs (Botta et al., 2021; Ferrocino et al., 2016). Characterization of beef microbiota from the early productive phases is therefore important to define its shelf-life the most suitable preventative strategy.

To understand at which level of accuracy the metataxonomic analyses can characterise and distinguish ground beef microbiota in relation to their origin prior grinding, two batches of beef burgers manufactured in the same production run were followed along their shelf-life and beyond. Bacterial and fungal community were investigated and comprehensively compared with culture-dependent microbiology and volatilomic profiles.

2. MATERIALS AND METHODS

2.1 Beef burger preparation and sampling

Beef burgers were manufactured in a local meat factory (Piedmont, Italy) with beef of *Fassona Piedmontese* cattle breed. Two batches (A and B) were prepared (trimming, grinding, packaging) consecutively the same day and in the same processing plant in February 2020: batches were provided from two different breeders, undergone independent slaughtering/maturation processes and no sanitization prior grinding. From each batch a total of 15 beef burgers (100 g each in a square shape)

were vacuum packed in a transparent linear low-density polyethylene bags (LLDPE; oxygen transmission, 0.83 $cm^3 \cdot m^{-2} \cdot h-1$ at 23 °C, 30 cm × 30 cm) and stored at 4.0 ± 0.5 °C without light exposure.

The expiration date was fixed by the producer the 14th day of vacuum storage at 4 °C in relation to previous shelf-life test performed following standard ISO indications for microbial analysis (ISO13721:1995, ISO 15214:1998, ISO 4833:2003). Three samples for each batch were analysed along five sampling points: the day 0, immediately after grinding-packaging; days 4 and 8, during regular shelf-life; days 15 and 30, after the expiration date.

2.2 Microbial counts

Serial dilutions were set up from ground beef samples (10 g of meat in 90 mL Ringer's solution; Oxoid) for each sampling point, with the exception of the the 30th day, due to the suspension of non-essential activities occurred during the pandemic emergency of March 2020.

Microbial counts were performed following standard ISO indications for the enumeration of spoilage population in meat products, without varying incubation parameters (temperature, oxygen) to favour the psychotrophic detection. This choice has been operated to resemble the common output obtained from analytical laboratories and metataxonomic analysis.

As far as viable population detected: Total Viable Count of mesophilic bacteria (TVC) on Plate Count Agar (PCA) incubated for 48 h at 30 °C; lactic acid bacteria (LAB) on De Man, Rogosa and Sharpe (MRS) agar incubated for 48 h at 30 °C in microaerophilic condition; coagulase-negative cocci (CNC) on Mannitol Salt Agar (MSA) incubated at 30 °C for 24 h; *Enterobacteriaceae* on Violet Red Bile Glucose Agar (VRBGA) incubated for 24 h at 37 °C; yeasts and moulds on Malt Extract agar (MEA) supplemented with tetracycline (0.05 g/L; Sigma-Aldrich, St. Louis, USA) and incubated at 25 °C for

five days. All media and supplements were provided by Biolife s.p.a. (Milan, Italy) unless differently stated. The pH of each sample was measured by using a digital pH-meter (Crison, Modena, Italy).

2.3 Analysis of volatile organic compounds (VOCs)

The volatile organic compounds (VOCs) in both batches of beef burger samples were determined in triplicate following the protocol suggested by Mentana and collegues (2019) slightly modified. The VOCs were extracted using headspace-solid phase microextraction (HS-SPME) and analysed by GC/MS (QP-2010 Plus, Shimadzu, Japan), interfaced with a computerized system for data acquisition (Software GC–MS Solution V. 2.5, Shimadzu, Japan). Briefly, 3.0 g of ground meat were accurately weighted in a 20 ml glass headspace vial with 20 µl of internal standard solution (1-octanol, 1.05 µg/mL) and sealed with a PTFE silicone septum. The VOCs were isolated by a fused-silica fibre (10 mm length) coated with a 50/30 mm thickness of DVB/CAR/PDMS and a Combi Pal system (CTC Analytics AG, Zwingen, Switzerland). The samples were conditioned at 40 °C for 15 min in order to reach the equilibrium; then, the fiber was exposed to headspace for 30 min. Next, the fiber was desorbed in split mode (split ratio 1:25) into the GC/MS injector at 248 °C for 5 min. The separation of VOCs was achieved using a Stabilwax column (20 m, 0.18 mm i.d., 0.18 µm film thickness, Restek, USA). Helium was used as carrier gas at constant linear velocity of 36.2 cm/sec, the oven temperature was from 40 °C (maintained for 4 min) to 210 °C by 5 °C/min, then increased up to 250 °C by 20 °C/min, the final temperature was held for 5 min. The ion source and interface temperature were set at 200 and 230 °C, respectively. The filament emission current was 70 eV and a mass range from 33 – 350 amu was scanned at 0.30 scan/s in scan mode. VOCs were recognized by comparing their mass spectra with those reported in the NIST08s (National Institute of Standards and Technology, Gaithersburg) library and pure commercial standards. In addition, the blank injection of fiber and vials were also carried out to prevent environmental

142 contamination. For quantitative purposes the response factor between the total ion current of each analyte
143 and internal standard was used to determine VOCs concentrations as μg/g.
144
145 **2.4 Amplicon-based sequencing**
146 At each sampling point, 1 ml of the first 10-fold serial dilution was collected, centrifuged at 13,000 rpm
147 for 30 s, the pellet was collected and stored at − 80 °C until DNA-extraction. Total DNA was extracted
148 from each sample collected as previously described (Ferrocino et al., 2016), standardized at 100 ng/L
149 (NanoDrop 1000 spectrophotometer; Thermo Scientific, Milan, Italy) and used to study the
150 metataxonomic profiles of bacterial and fungal microbiota in parallel. Amplicon library of V3-V4 region
151 was constructed from 16S rRNA gene of bacterial DNA using primers and conditions previously reported
152 (Klindworth et al., 2013), while amplicon library of the D1 domain from 26S rRNA gene of fungal Large
153 Ribosomal Subunit (LSU) was prepared with primers and conditions described by (Mota-Gutierrez,
154 Ferrocino, Rantsiou, & Cocolin, 2019).
155 The PCR products of both libraries were purified with Agencourt AMPure kit (Beckman Coulter, Milan,
156 Italy) and the resulting products were tagged with sequencing adapters using the Nextera XT library
157 preparation kit (Illumina Inc, San Diego, CA), according to the manufacturer's instructions. Sequencing
158 was performed using a MiSeq Illumina instrument (Illumina) with V3 chemistry, which generated 2 X
159 250 bp paired-end reads. MiSeq Control Software, V2.3.0.3, RTA, v1.18.42.0, and CASAVA, v1.8.2,
160 were used for the base-calling and Illumina barcode demultiplexing processes.
161
162 **2.5 Bioinformatic analysis**
163 A total of 570,943 and 1,673,760 raw-reads were respectively produced by 16S and 26S amplicon-based
164 sequencing of the thirty samples collected. To obtain Amplicon Sequence Variants (ASVs) the raw-reads

were analysed with *DADA2* package in R environment (Callahan et al., 2016), using R program for Statistical Computing 4.1.1 (http://www.r-project.org).

For 16S amplicon-based sequencing, 325,271 reads passed the quality filtering parameters applied [*truncLen=c(250,222); trimLeft = c(35,35); maxEE=c(2,2); minLen = c(50,50)*] with an average value of 10,842 reads/sample. After merging (minimum overlap of 5 bp) and *de-novo* chimera removal (*per-sample* method) all paired-end sequences shorter than 365 bp were discharged: 89.1 % of the initial filtered sequences were used to construct bacterial ASVs frequency table. For 26S fungal gene, filtering parameters [*truncLen=c(245,240); trimLeft = c(35,35); maxEE=c(2,2); minLen = c(50,50)*] reduced the reads to 1,185,674 (40,781 reads/sample in average). After merging (minimum overlap of 12 bp) and *de-novo* chimera removal (*per-sample* method) no trimming was performed in relation to the length variability of this amplified region; one sample of production B collected from the fifteenth day was removed due to low sequences number (< 1000). Finally, 54.2 % of the initially filtered sequences were used to construct fungal ASVs frequency table. All parameters not reported for filtering/merging steps are intended as default *DADA2* setting.

Taxonomy was assigned with a 99 % sequence similarity through Bayesian classifier method (Wang, Garrity, Tiedje, & Cole, 2007) by matching bacterial ASVs to the 2021 release (version 138.1) of Silva prokaryotic SSU reference database (https://zenodo.org/record/4587955#.YObFvhMzZRE), with a further check at 100 % of similarity for ASVs assigned to the species level with the *addSpecies* script. Fungal ASVs taxonomy was assigned at 99 % against an internal database of 26S rRNA (Mota-Gutierrez et al., 2019), then confirmed against NCBI LSU-reference database by using BLASTn suite (https://www.ncbi.nlm.nih.gov/nuccore?term=PRJNA51803). When the taxonomic assignment was not able to reach the species, the highest taxonomic level available was displayed. ASVs with uncertain taxonomic assignment (to the Order rank or lower resolution) were aligned against NCBI nucleotide collection (https://www.ncbi.nlm.nih.gov/) and all sequences matching (> 99 % similarity) vegetable

189 genomes (mainly pepper), animal genomes (meat), mitochondria and chloroplasts were removed from
190 the frequency tables.
191 ASVs were aligned with PyNAST (Caporaso et al., 2010) and unrooted phylogenetic trees were
192 constructed with FastTree (Price, Dehal, & Arkin, 2009) to allow further phylogenetic based analysis.
193 Alpha diversity metrics (Observed Species, ACE, Shannon, Simpson, Fisher, PD whole tree) and
194 weighted UniFrac beta-diversity distance were calculated with *phyloseq* and *picante* packages (Kembel
195 et al., 2010; McMurdie & Holmes, 2013): rarefaction limit was set to the lowest number of
196 sequences/sample.
197 Metagenome inference was performed from bacterial ASVs frequency table with MetGEMs toolbox
198 (Patumcharoenpol et al., 2021) using default parameters (https://github.com/yumyai/MetGEMs) and
199 AGORA collection as reference database of genome-scale models (Magnúsdóttir et al., 2017). Gene
200 family abundances were predicted and identified as KEGG orthologs (KO) and collapsed at level 3 of
201 the KEGG annotations.
202 Sequencing data were deposited at the Sequence Read Archive of the National Center for Biotechnology
203 Information under the bioproject accession number PRJNA777553.
204
205 **2.6 Statistics**
206 Statistical analyses and data plotting were performed in R environment unless otherwise stated. Normality
207 and homogeneity of the data (Log-Transformed abundances, alpha-diversity metrics, viable counts,
208 VOCs concentrations) were checked by means of Shapiro-Wilk's W and Levene's tests, respectively.
209 Variation and differences between multiple groups were assessed with one-way ANOVA (coupled with
210 Tukey's post-hoc test) and Kruskal–Wallis's test (coupled with pairwise Wilcoxon's test) for parametric
211 and not parametric data, respectively. Pairwise comparisons were alternatively performed with Wilcoxon
212 and T-tests according to data normality.

213 Principal Component Analysis (PCA) was performed on VOCs concentrations with *factominer* package.
214 Adonis and ANOSIM statistical tests were used to detect significant differences among VOCs (PCA
215 scores) and microbial communities (PCoA based on β-diversity weighted UniFrac distance). Non-metric
216 Multi-Dimensional Scaling (NMDS) analyses were based on Bray-Curtis dissimilarities and were
217 performed by using original ASVs frequency tables as input. The significance influence of time and batch
218 (individually or interactively) on clusters produced by NMDS was tested by Permutation Analysis of
219 Variance (PERMANOVA), using the *Adonis* function based on Brey-Curtis dissimilarity distance. Best
220 set of taxa and VOCs that were significantly fitting (Pearson's moment correlation; Bray-Curtis distance)
221 with the NMDS-based distribution of the samples were calculated by *bioenv* function and plotted in the
222 NMDS bi-plot as vectors (Torondel et al., 2016).
223 To construct the ASVs co-occurrence/exclusion network, the SparCC algorithm was run with default
224 parameters and 100 bootstraps using the package *SpiecEasi* (Friedman & Alm, 2012). Pseudo *P*-values
225 were calculated as the proportion of simulated bootstraps and only highly significant (pseudo *P*-values <
226 0.001) positive ($R > 0.5$) and negative ($R < -0.5$) correlations were used to infer the network with the
227 program Gephi 0.9.2-beta (https://gephi.org). Presence of recurrent sub-networks modules (group of
228 ASVs that are co-varying) were detected considering only co-occurrences through the modularity
229 algorithm implemented in Gephi suite with default parameters (Blondel, Guillaume, Lambiotte, &
230 Lefebvre, 2008). Correlation between taxa (ASVs merged at highest taxonomic level achieved) and
231 VOCs concentration was performed by means of Spearman's rank correlation.
232 Enrichment analysis was performed with *GAGE* package on the predicted KO abundance table to identify
233 biological pathways significantly overrepresented and underrepresented between batches (Luo,
234 Friedman, Shedden, Hankenson, & Woolf, 2009).
235
236 **3. RESULTS**

3.1 Microbiological dynamics

No differences were observed in microbiological dynamics between batches A and B by comparing each single sampling point at 0, 4, 8 and 15 days, although in batch B we observed the tendency to reach higher counts the fifteenth day (**Fig. 1**). As far as the time-dependent growth, in both batches TVC and LAB counts increased significantly (Kruskal-Wallis; $P< 0.05$) from day 0 to the eighth day with a progressive growth of 3 logarithms. On the other hand, yeast counts increased significantly from the fourth to the eighth day (~ 1.5 Log CFU/g increase), whereas the *Enterobacteriaceae* population showed a marked growth from eighth to the fifteenth day ($P< 0.05$). The pH value remained stable along the first fifteen days of storage, with an average value of pH 5.52 ± 0.12 (**data not shown**).

3.2 Metabolomic biomarkers of spoilage

A total of fifty-two VOCs were quantified in the headspace of beef burger packages along the 30 days of storage monitored (**Supplementary Table 1**). Alcohols represented the more abundant compounds (10.3 ± 5.2 μg/g in average), followed by aldehydes (7.0 ± 5.0 μg/g), ketones (2.0 ± 1.1 μg/g), organic acids (1.5 ± 1.2 μg/g) and alkanes (1.1 ± 0.7 μg/g). Less abundant VOCs were represented by esters (mainly ethyl acetate), aromatic compounds (indole) and one lactam (caprolactam). Changes in the volatilomic profile were mainly related to storage time, with some VOCs that showed different dynamics between batches. In particular, along the shelf-life of batch A the amounts of hexanal, isopropyl alcohol and the acetic/formic acids decreased significantly (ANOVA and Tukey's post hoc; $P < 0.05$) after the fourth day, while butanoic and propanoic acids concentrations increased after the eighth day. Less time-dependent variability was observed in batch B, were only three VOCs (1-pentanol, 2-heptenal, ethyl-cyclopentane) decreased progressively and significantly along the 30 day of vacuum storage. In both batches, ethanol, 3-methyl-1-butanol, ethyl acetate and caprolactam showed the highest concentrations

261 the thirteenth day, whereas 1-octel-3-ol significantly decreased at the end of storage. Moreover,
262 comparing the volatilomes profile of the batches in each single day we observed that several VOCs
263 (pentanal, 2-butanone, acetoin, acetone, ethyl-cyclopentane, 3-methyl- heptane, ethyl acetate) were
264 significantly (T-test; $P < 0.01$) more abundant in batch B the eighth and fifteenth day.
265 Principal Component Analysis (PCA) confirmed that time had a greater impact on data variance in
266 comparison to the effect exerted by the batches. Indeed, scores plots show a significant (Anosim and
267 ADONIS tests; $P < 0.001$) separation of the thirtieth day samples from all the others (**Fig 2 A**).
268 Considering that the two first PCA dimensions explained 47.8 % of the variance, the discrimination of
269 the samples along time is mainly led by the first dimension (Dim1), with the second dimension (Dim2)
270 related to the minimal and not significant segregation of the samples between batches (**Fig 2 B**). The
271 corresponding loading plot of the variables shows that alkanes and aldehydes/alcohols are the main
272 VOCs that contribute to the variance explained by the first and second dimensions, respectively (**Fig 2**
273 **C and D**).
274
275 **3.3 Compositional changes in bacterial and fungal communities during shelf-life**
276 Bacterial community of beef burgers was mainly formed by members of Firmicutes phylum, namely
277 *Leuconostoc gelidum*, *Dellaglioa sp*., *Carnobacterium divergens*, *Latilactobacillus sp*., *Streptococcus*
278 *salivarius*, *Lactococcus piscium*, *Kocuria rhizophila* and different species belonging to *Staphylococcus*
279 (**Fig 3 A**). Gram negative bacteria were less abundant and primarily represented by *Bacteroides sp*. and
280 the psychrophiles *Pseudomonas fragi*/*psychrophila*, in the early and late stages of storage respectively.
281 Through the Permutational Analysis of Variance (PERMANOVA; **Supplementary Table 2)** we
282 observed that the greatest portion of variability in the microbiota composition was determined by the
283 batch (R^2=0.122; $P < 0.01$), while the time explained a lower portion of variability and not significantly
284 (R^2=0.104; P>0.05). Independently from time, batch B was characterized by greater (P[FDR] <0.05)

richness, diversity and an overall higher (*P*[FDR] <0.001) presence of *Lactococcus piscium*, *Carnobacterium divergens*, *Pseudomonas psychrophila* and *Pseudomonas fragi* abundances, in comparison to batch A (**Supplementary Figure 1**). Moreover, we observed during vacuum storage of the batches different succession patterns of the main species, more easily appreciated by dividing the period in three storage phases (**Fig 3 B**): hamburgers at day 0, shortly after production and packaging (named "Production"); within the use-by date (day 4 and 8 collectively named "Shelf-life"); and after the use-by date (day 15 and 30 collectively named "Expired"). In particular, ASVs assigned to *Leuconostoc gelidum, Carnobacterium divergens* and *Dellagliola* sp. were not detected the first day. On the contrary, *Streptococcus*, *Staphylococcus* and *Kokuria* were highly abundant the first day and not anymore present after the fourth day of storage. Interestingly, the disappearance of initially dominating taxa, like *Staphylococcus* and *Kokuria*, was less significant and more gradual in batch B, in which we observed after the use-by date a greater increase of *Lactococcus piscium* and an undefined *Lactobacillus* species included in the new *Latilactobacillus* genus. However, β-diversity analysis (**Fig 3 C)** showed that beef burgers immediately after production (day 0) represented in both batches a phylogenetically distinct community (weighted UniFrac distance; ADONIS and Anosim: *P*[FDR] <0.001) compared to all the following sampling points (days 4, 8, 15 and 30).

As far as fungi are concerned, we observed a core mycobiota composed by nine yeasts and three molds, which represented together more than 50 % of total abundance in 70 % of the samples (**Figure 4**). In particular, *Kurtzmaniella zeylanoides* and *Debaryomyces hansenii* were the most abundant yeasts and were present in all samples, followed by less ubiquitous ASVs assigned to the *Trichosporonaceae* family (*Trichosporon*, *Apiotrichum*) and to the genera *Starmerella*, *Cutaneotrichosporon* and *Malassezia*. Filamentous fungi were mainly represented by *Cladosporium cladosporioides, Penicillium* sp. and, to a lesser extent, *Phanerochaete australosanguinea*. As far as compositional variability of the mycobiota, PERMANOVA did not highlight any significant effect of time and batch (**Supplementary Table 2**).

309 Accordingly, no significant differences in the distribution of the main taxa and alpha-diversity measures
310 were observed between batches, along the time course and in relation to the three phases aforementioned.
311
312 **3.4 Correlation patterns of bacterial and fungal communities**
313 In order to display and better understand the ecological associations determined by the succession
314 patterns observed, a co-occurrence/exclusion network was inferred using the significant SparCC
315 correlations (*P*-value < 0.001) existing among the core bacteria and fungi, at the level of each unique
316 ASV (**Fig. 5 A**).
317 The correlation network shows 45 nodes composed by 27 bacterial- and 18 fungal-ASVs, respectively;
318 these nodes are connected by 161 edges, of which 120 represent positive correlation. The majority of the
319 remaining 41 negative correlations were observed between ASVs of the same kingdom. Bacteria related
320 to the initial meat contamination, such as *Staphylococcus*, *Kokuria* and *Streptococcus*, were negatively
321 correlated to ASVs that were predominant from the fourth day of vacuum storage, namely *Dellaglioa*,
322 *Leuconostoc, Carnobacterium* and *Latilactobacillus*. Within fungi, ASVs assigned to *Kurtzmaniella*
323 *zeylanoides* and *Kurtzmaniella santamariae* showed the higher number of negative correlations with the
324 other yeasts and moulds and several positive correlations with the bacterial ASVs of *Dellaglioa*,
325 *Leuconostoc* and *Latilactobacillus* (**Supplementary Table 3**).
326 Taking into account only the co-occurrences (**Fig. 5 B**), five modules of highly co-occurring ASVs were
327 identified. The modules coded as 2 and 3 encompass the initial mycobiota and microbiota of hamburgers,
328 respectively, whereas the closely related modules 0 and 1 comprise all ASVs that dominated the
329 microbiota and mycobiota of hamburgers from the fourth to the thirteenth day. Notably, the bacterial
330 ASVs grouped in the module 0 are distinctive of the batch B (**Fig. 5 C**).
331
332 **3.5 Links between volatilomic profiles and microbiota composition**

To depict the significant batch-to-batch variation of the bacterial community, non-metric multidimensional scaling (NMDS) based on core species (> 0.5 % average abundance) was performed (**Fig. 6**). NMDS ordination was not plotted for the fungal community in relation to the not significant influence of batches and time on its distribution.

In addition to the NMDS ordination of the samples, VOCs and bacterial taxa significantly correlated (Pearson's correlation; $P < 0.001$) with the bacterial community variance were plotted as arrows, of which vertexes represent the direction of change of each VOC and taxa (**Fig. 6 and Supplementary Table 4**). The presence of *Kokuria rhizophila* and formic acid was markedly related to the moment of packaging (day 0) in both batches. Acetoin, indole and hexanal were correlated to batch B, and in particular to its shelf-life period (days 4 and 8), while benzenacetaldheyde was mostly correlated with the expired samples of this batch (from 15 to 30 days). As far as the bacterial species are concerned, the separation between samples of the two batches was highly correlated to the presence of *Carnobacterium divergens* and the duo *Dellagliola sp.*/*Leuconostoc gelidum* in batch A and B, respectively. Moreover, NMDS plot highlighted the gradual change of microbiota composition in batch B during early stages (from 0 to 4 days), in comparison to A in which it is graphically more marked.

Concerning the direct pairwise correlations between bacteria/fungi abundances and VOCs concentration, we observed that the pattern of positive and negative correlations (P[FDR]<0.001) were highly dependent of the time course (**Supplementary Figure 2**). Indeed, all dominant taxa in the early stages of storage (Bacteria: *Kokuria, Staphylococcus, Streptococcus*; Fungi: *Cladosporium, Apiotrichum*) were positively correlated with the VOCs mostly present at day 0, such as hexanal, 1-pentanol, acetic and formic acid. On the contrary, the most abundant taxa *Leuconostoc gelidum* and *Kurtzmaniella zeylanoides*, which have developed after the fourth day, were negatively correlated with theses VOCs.

3.6 Functional differences in the inferred microbiome

The majority of the metabolic pathways differentially represented (*GAGE* enrichment statistic: $P < 0.001$) between the two batches belonged to the carbohydrate metabolism (**Supplementary Figure 3).** In particular, five pathways related to the monosaccharides/polysaccharide metabolisms (ko00052, ko00500, ko00051, ko00040) and the central pathway of glycolysis/gluconeogenesis (ko00010) were presumptively overrepresented in A and underrepresented in B. In parallel, the TCA cycle (ko00020), the pathways of glyoxylate/dicarboxylate metabolism (ko00630), and two pathways responsible of butyric and propionic acids production (ko00640, ko00650) were likely overrepresented in B.

Abundance differences of metabolic pathways related to amino acid metabolisms were observed as well, with valine/leucine/isoleucine degradation (ko00280) and β-alanine metabolism presumptively enriched in B, and an overall higher biosynthesis of amino acids (ko01230) histidine-glutathione metabolisms (ko00340, ko00480) predicted in the batch A. Finally, lipopolysaccharide biosynthesis (ko00540) was enriched in B, while conversely the glycerophospholipid metabolism (ko00564) was presumptively more abundant in A.

4. DISCUSSION

Metataxonomic has already proved capable to characterize and clearly distinguish ground beef microbiota among different production runs (Botta et al., 2021; Sade, Penttinen, Björkroth, & Hultman, 2017). Deeping the potentiality of this culture-independent analysis, here the possibility to microbiologically discriminate between beef burger batches manufactured in the same processing run but from different pre-grinding origin has been explored.

The two batches studied have shown the same microbial counts along time course, likely in reason of the same initial contamination level and storage conditions. As expected in a vacuum packaged meat, LAB population constituted the majority of the culturable fraction from the early storage stages (Ercolini, Russo, Torrieri, Masi, & Villani, 2006; Pothakos et al., 2015), and reached a microbial spoilage threshold

capable to cause sensory deterioration already the eighth day (Stoops et al., 2015). On the basis of stationary phase reached , we could assume that both batches were already in the early spoilage condition at the end of the first week (Hultman et al., 2020).

On the other hand, metataxonomic analysis highlighted from the fourth day a marked discrepancy between batches of most abundant taxa, mainly represented by psychrotrophic LAB species, which are generally recognized as meat spoilers and usually underestimated by mesophilic enumeration protocols (Jääskeläinen et al., 2015; Pennacchia et al., 2011; Pothakos et al., 2014; Stoops et al., 2015). Despite we are aware that different incubation conditions would have potentially provide different LAB dynamics, a distinction between the microbial composition of batches would have not be effective if not coupled with a massive isolation and identification of the colonies (Pothakos et al., 2014). Moreover, due to the advancement of new technologies, the current time to execute metataxonomic analysis are comparable to those of a complete culture-based characterization of microbiota (Jagadeesan et al., 2019; Rhoads & Au, 2015; van Dijk, Jaszczyszyn, Naquin, & Thermes, 2018). Therefore, metataxonomic analysis demonstrated in the present study to provide a better discriminatory capability than culture-dependent approaches.

Aside the comparison between culture-dependent and -independent outputs, we observed through metataxonomic analysis a temporal succession of species in both bacterial and fungal ecologies. While time course succession of spoilage bacteria has been widely observed during cold storage of packaged meat , no information is available on mycobiota development in ground beef during its cold-vacuum storage (Jääskeläinen, Hultman, Parshintsev, Riekkola, & Björkroth, 2016; Sade et al., 2017). Indeed, the numerous culture-independent surveys carried out on cured meats are not directly comparable in reason to significantly higher temperatures (Alapont, Martínez-Culebras, & López-Mendoza, 2015; Alía et al., 2016; Belleggia et al., 2020; Franciosa et al., 2021). Our observation and the mycobiota dynamics described in dry cold-aged beef indicate that a longitudinal succession of yeast species can occur also

405 during meat cold storage, and it is generally characterised by an increasing presence of *Kurtzmaniella*
406 *zeylanoides* along time course (Oh et al., 2019; Ryu et al., 2018). However, the weak increase of yeast
407 and mold counts showed their inability to actively affect beef burgers spoilage, confirming previous
408 observations in tray-packaged pork during cold storage (Yang et al., 2017).
409 Immediately after packaging, bacterial and fungal communities were composed in both batches by genera
410 and species that commonly inhabit the processing plant environment and can colonise meat during each
411 processing run (Botta et al., 2020; Chaillou et al., 2015; Kang, Ravensdale, Coorey, Dykes, & Barlow,
412 2019). In particular, several species of *Staphylococcus* and *Streptococcus*, as well as fungi like
413 *Malassezia*, *Trichosporon* and *Cutaneotrichosporon*, are well known members of human/animal skin,
414 nostrils and mouth (Cundell, 2018; Zhang et al., 2020). On the other hand, *Kocuria* spp. and filamentous
415 fungi (*Cladosporium, Penicillium*) were more probably transported on meat contact surfaces by dust and
416 air (Chaillou et al., 2015). A distinguishing composition of bacterial community at the moment of
417 production-packaging have already been observed during packaged beef shelf-life and associated to
418 different production days (Sade et al., 2017).
419 Noteworthy, this initial autochthonous community has here represented a transitory signature of the
420 production run shared by the two batches. Indeed, it has been soon replaced by other batch-
421 autochthonous species likely collected on the carcases and cuts during the previous slaughtering-boning
422 phases carried out in the supplier's facilities (Kang et al., 2019). This second community was mainly
423 composed by psychotrophic LAB suited to develop during shelf-life and to cause the product spoilage
424 (Pothakos et al., 2015). The parallel logarithmic increase of LAB counts confirms the predominance of
425 this population over the rest of spoilage microbiota, in spite of the aforementioned culture-dependent
426 underestimation of psychrotrophs.
427 Not only bacteria distribution and abundances differed between batches, but also their temporal
428 succession patterns did. *Leuconostoc gelidum* and *Dellagliola sp*. took simultaneously and sharply over

429 the dominance after packaging in batch A, and remained predominant until the thirtieth day. On the
430 contrary, *Carnobacterium divergens* become the predominant species in batch B until the eighth day,
431 from which onwards a remarkable presence of *Lactococcus piscium* and *Pseudomonas spp* was observed.
432 The occurrence of *Pseudomonas spp*. in the late vacuum storage phases and a more heterogeneous
433 production of VOCs, with some concentrations over the threshold of sensory perception, indicates a
434 faster spoilage dynamic for the batch B in comparison to A (Casaburi et al., 2015; Ercolini et al., 2011).
435 This worst-case scenario in batch B is likely connected to the dynamic and rapid succession of spoilage
436 bacteria occurred during its vacuum storage.
437 Focusing on VOCs production, high concentrations of acetoin were observed in the second week of B
438 storage. The accumulation of this buttery-odour compound in vacuum packaged meat can be the result
439 of *Carnobacterium divergens* homofermentative metabolism or the catabolism of aspartate and alanine
440 by *Lactococcus piscium*: both predominant in this batch (Andreevskaya et al., 2018; Höll, Hilgarth,
441 Geissler, Behr, & Vogel, 2020). In particular, acetoin production by *Lactococcus piscium* take place in
442 the late stages of vacuum meat storage when glucose has been consumed by other fast-growing LAB
443 able to upregulate carbohydrate pathways, such as the *Leuconostoc gelidum* that was dominant in batch
444 A (Andreevskaya et al., 2018; Hultman et al., 2020). Noteworthy, metabolic pathways related to
445 monosaccharides and amino acids catabolisms were presumptively more abundant in batch A and B,
446 respectively.
447 Moreover, *Lactococcus piscium* is the main meat spoilage LAB in low oxygen conditions in which
448 represents an endpoint indicator of shelf-life, while in presence of oxygen the *Leuconostoc gelidum* is
449 favoured by its heme-dependent respiration capability (Botta et al., 2021; Jääskeläinen et al., 2016;
450 Rahkila, Nieminen, Johansson, Säde, & Björkroth, 2012). Different factors from the gaseous composition
451 have therefore alternatively boosted the development of these two species two vacuum packaged batches;
452 for instance the presence of more or less mutualistic species in the original batch-autochthonous

453 microbiota. Co-occurrence analysis has indeed suggested a limited ecological coexistence in these
454 batches between *Lactococcus piscium* and *Leuconostoc gelidum*. On the contrary, a better level of
455 coexistence seems to exist between *Leuconostoc gelidum* and *Dellagliola*, another predominant spoilage
456 species in low oxygen conditions (Jääskeläinen et al., 2016). Bearing in mind that inferred correlations
457 among abundances may not directly reflect the real ecological interactions, further physiological
458 confirmation of the co-occurrences observed are undoubtedly needed (Faust & Raes, 2012; Hirano &
459 Takemoto, 2019).
460 To conclude, this study showcases that metataxonomic-based profiling of meat microbiota represents an
461 effective approach to recognize in each production run the batches of different origin. In parallel we
462 showed that final production phases like trimming and grinding seems to produce transitory modification
463 of the autochthonous microbiota previously collected on carcasses and cuts. Although this is still a proof
464 of concept, the discriminatory potentiality of metataxonomic analysis has been here proved. In this light,
465 the characterisation of each beef batch microbiota in the early productive stages and its association with
466 the derived products spoilage fate will allow to create in future studies a benchmark database of those
467 profiles that can alternatively reduce or extend the final product shelf-life. This further advancement
468 would finally make the metataxonomic analysis an usable and practical tool for food industries.
469
470
471 **ACKNOWLEDGEMENTS**
472
473 **AUTHOR CONTRIBUTIONS**
474 Ilario Ferrocino and Luca Cocolin designed and conceptualized the experiment. Irene Franciosa,
475 Vladimiro Cardenia and Valentina Alessandria performed microbiological and chemical analysis. Ilario
476 Ferrocino performed amplicon-based sequencing. Cristian Botta carried out the bioinformatic analysis,

statistics, data interpretation, generated the manuscript figures and wrote the original draft. Irene Franciosa Ilario Ferrocino and Luca Cocolin supervised the data analysis and contributed to manuscript preparation. All authors revised and approved the final version of the manuscript.

REFERENCES

Alapont, C., Martínez-Culebras, P. V., & López-Mendoza, M. C. (2015). Determination of lipolytic and proteolytic activities of mycoflora isolated from dry-cured teruel ham. *Journal of Food Science and Technology*, *52*(8), 5250–5256. https://doi.org/10.1007/s13197-014-1582-5

Alía, A., Andrade, M. J., Rodríguez, A., Reyes-Prieto, M., Bernáldez, V., & Córdoba, J. J. (2016). Identification and control of moulds responsible for black spot spoilage in dry-cured ham. *Meat Science*, *122*, 16–24. https://doi.org/10.1016/j.meatsci.2016.07.007

Andreevskaya, M., Auvinena, P., Jääskeläinen, E., Johansson, P., Ylinen, A., Paulin, L., … Auvinena, P. (2018). Food Spoilage-Associated Leuconostoc, Lactococcus, and Lactobacillus Species Display Different Survival Strategies in Response to Competition. *Applied and Environmental Microbiology*, *84*, 1–16. https://doi.org/10 .1128/AEM.00554-18

Bao, Y., Puolanne, E., & Ertbjerg, P. (2016). Effect of oxygen concentration in modified atmosphere packaging on color and texture of beef patties cooked to different temperatures. *Meat Science*, *121*, 189–195. https://doi.org/10.1016/J.MEATSCI.2016.06.014

Belleggia, L., Ferrocino, I., Reale, A., Boscaino, F., Di Renzo, T., Corvaglia, M. R., … Osimani, A. (2020). Portuguese cacholeira blood sausage: A first taste of its microbiota and volatile organic compounds. *Food Research International*, *136*(July). https://doi.org/10.1016/j.foodres.2020.109567

Blondel, V. D., Guillaume, J. L., Lambiotte, R., & Lefebvre, E. (2008). Fast unfolding of communities in large networks. *Journal of Statistical Mechanics: Theory and Experiment*, *10*, 1–12.

https://doi.org/10.1088/1742-5468/2008/10/P10008

Bonnet, C., Bouamra-Mechemache, Z., Réquillart, V., & Treich, N. (2020). Viewpoint: Regulating meat consumption to improve health, the environment and animal welfare. *Food Policy*, *97*(February), 101847. https://doi.org/10.1016/j.foodpol.2020.101847

Botta, C., Coisson, J. D., Ferrocino, I., Colasanto, A., Pessione, A., Cocolin., L., … Rantsiou, K. (2021). Impact of electrolyzed water on the microbial spoilage profile of Piedmontese steak tartare. *Microbiology Spectrum*, *9*(3), e01751-21. https://doi.org/doi.org/10.1128/Spectrum.01751-21

Botta, C., Ferrocino, I., Cavallero, M. C., Riva, S., Giordano, M., & Cocolin, L. (2018). Potentially active spoilage bacteria community during the storage of vacuum packaged beefsteaks treated with aqueous ozone and electrolyzed water. *International Journal of Food Microbiology*, (June), 10–12. https://doi.org/10.1016/j.ijfoodmicro.2017.10.012

Botta, C., Ferrocino, I., Pessione, A., Cocolin, L., & Rantsiou, K. (2020). Spatiotemporal Distribution of the Environmental Microbiota in Food Processing Plants as Impacted by Cleaning and Sanitizing Procedures: The Case of Slaughterhouses and Gaseous Ozone. *Applied and Environmental Microbiology*, *86*(23), 1–15. https://doi.org/10.1128/aem.01861-20

Callahan, B. J., McMurdie, P. J., Rosen, M. J., Han, A. W., Johnson, A. J. A., & Holmes, S. P. (2016). DADA2: High-resolution sample inference from Illumina amplicon data. *Nature Methods*, *13*(7), 581–583. https://doi.org/10.1038/nmeth.3869

Caporaso, J. G., Bittinger, K., Bushman, F. D., Desantis, T. Z., Andersen, G. L., & Knight, R. (2010). PyNAST: A flexible tool for aligning sequences to a template alignment. *Bioinformatics*, *26*(2), 266–267. https://doi.org/10.1093/bioinformatics/btp636

Casaburi, A., Piombino, P., Nychas, G. J., Villani, F., & Ercolini, D. (2015). Bacterial populations and the volatilome associated to meat spoilage. *Food Microbiology*, *45*(PA), 83–102.

https://doi.org/10.1016/j.fm.2014.02.002

Chaillou, S., Chaulot-Talmon, A., Caekebeke, H., Cardinal, M., Christieans, S., Denis, C., … Champomier-Vergès, M.-C. (2015). Origin and ecological selection of core and food-specific bacterial communities associated with meat and seafood spoilage. *The ISME Journal*, *9*(5), 1105–1118. https://doi.org/10.1038/ismej.2014.202

Cundell, A. M. (2018). Microbial Ecology of the Human Skin. *Microbial Ecology*, *76*(1), 113–120. https://doi.org/10.1007/s00248-016-0789-6

de Filippis, F., La Storia, A., Villani, F., & Ercolini, D. (2013). Exploring the Sources of Bacterial Spoilers in Beefsteaks by Culture-Independent High-Throughput Sequencing. *PLoS ONE*, *8*(7), e70222. https://doi.org/10.1371/journal.pone.0070222

De Filippis, F., Parente, E., & Ercolini, D. (2018). Recent Past, Present, and Future of the Food Microbiome. *Annual Review of Food Science and Technology*, *9*, 589–608. https://doi.org/10.1146/annurev-food-030117-012312

Ercolini, D., Ferrocino, I., Nasi, A., Ndagijimana, M., Vernocchi, P., La Storia, A., … Villani, F. (2011). Monitoring of Microbial Metabolites and Bacterial Diversity in Beef Stored under Different Packaging Conditions. *Applied and Environmental Microbiology*, *77*, 7372–7381. https://doi.org/10.1128/aem.05521-11

Ercolini, D., Russo, F., Torrieri, E., Masi, P., & Villani, F. (2006). Changes in the spoilage-related microbiota of beef during refrigerated storage under different packaging conditions. *Applied and Environmental Microbiology*, *72*(7), 4663–4671. https://doi.org/10.1128/AEM.00468-06

Faust, K., & Raes, J. (2012). Microbial interactions: From networks to models. *Nature Reviews Microbiology*, *10*(8), 538–550. https://doi.org/10.1038/nrmicro2832

Ferrocino, I., Greppi, A., Lastoria, A., Rantsiou, K., & Ercolini, D. (2016). *Impact of Nisin-Activated Packaging on Microbiota of Beef Burgers during Storage*. *82*(2), 1–13.

549 https://doi.org/10.1128/AEM.03093-15.Editor
550 Franciosa, I., Coton, M., Ferrocino, I., Corvaglia, M. R., Poirier, E., Jany, J. L., … Mounier, J. (2021).
551 Mycobiota dynamics and mycotoxin detection in PGI Salame Piemonte. *Journal of Applied*
552 *Microbiology*. https://doi.org/10.1111/jam.15114
553 Friedman, J., & Alm, E. J. (2012). Inferring Correlation Networks from Genomic Survey Data. *PLoS*
554 *Computational Biology*, *8*(9), 1–11. https://doi.org/10.1371/journal.pcbi.1002687
555 Grispoldi, L., Karama, M., Sechi, P., Iulieto, M. F., & Cenci-Goga, B. T. (2020). Effect of the addition
556 of starter cultures to ground meat for hamburger preparation. *Microbiology Research*, *11*(1).
557 https://doi.org/10.4081/mr.2020.8623
558 Hirano, H., & Takemoto, K. (2019). Difficulty in inferring microbial community structure based on co-
559 occurrence network approaches. *BMC Bioinformatics*, *20*(1), 1–14.
560 https://doi.org/10.1186/s12859-019-2915-1
561 Höll, L., Hilgarth, M., Geissler, A. J., Behr, J., & Vogel, R. F. (2020). Metatranscriptomic analysis of
562 modified atmosphere packaged poultry meat enables prediction of Brochothrix thermosphacta and
563 Carnobacterium divergens in situ metabolism. *Archives of Microbiology*, *202*(7), 1945–1955.
564 https://doi.org/10.1007/s00203-020-01914-y
565 Hultman, J., Johansson, P., & Björkroth, J. (2020). Longitudinal Metatranscriptomic Analysis of a
566 Meat Spoilage Microbiome Detects Abundant Continued Fermentation and Environmental Stress
567 Responses during Shelf Life and Beyond. *Applied and Environmental Microbiology*, *86*(24), 1–
568 15. https://doi.org/10.1128/AEM.01575-20
569 Jääskeläinen, E., Hultman, J., Parshintsev, J., Riekkola, M. L., & Björkroth, J. (2016). Development of
570 spoilage bacterial community and volatile compounds in chilled beef under vacuum or high
571 oxygen atmospheres. *International Journal of Food Microbiology*, *223*, 25–32.
572 https://doi.org/10.1016/j.ijfoodmicro.2016.01.022

573 Jääskeläinen, E., Vesterinen, S., Parshintsev, J., Johansson, P., Riekkola, M. L., & Björkroth, J. (2015).
574 Production of buttery-odor compounds and transcriptome response in Leuconostoc gelidum subsp.
575 gasicomitatum LMG18811T during growth on various carbon sources. *Applied and*
576 *Environmental Microbiology*, *81*(6), 1902–1908. https://doi.org/10.1128/AEM.03705-14
577 Jagadeesan, B., Gerner-Smidt, P., Allard, M. W., Leuillet, S., Winkler, A., Xiao, Y., … Grant, K.
578 (2019). The use of next generation sequencing for improving food safety: Translation into
579 practice. *Food Microbiology*, *79*(October 2018), 96–115. https://doi.org/10.1016/j.fm.2018.11.005
580 Kang, S., Ravensdale, J., Coorey, R., Dykes, G. A., & Barlow, R. (2019). A Comparison of 16S rRNA
581 Profiles Through Slaughter in Australian Export Beef Abattoirs. *Frontiers in Microbiology*,
582 *10*(November), 1–10. https://doi.org/10.3389/fmicb.2019.02747
583 Kembel, S. W., Cowan, P. D., Helmus, M. R., Cornwell, W. K., Morlon, H., Ackerly, D. D., … Webb,
584 C. O. (2010). Picante: R tools for integrating phylogenies and ecology. *Bioinformatics*, *26*(11),
585 1463–1464. https://doi.org/10.1093/bioinformatics/btq166
586 Klindworth, A., Pruesse, E., Schweer, T., Peplies, J., Quast, C., Horn, M., & Glöckner, F. O. (2013).
587 Evaluation of general 16S ribosomal RNA gene PCR primers for classical and next-generation
588 sequencing-based diversity studies. *Nucleic Acids Research*, *41*(1), 1–11.
589 https://doi.org/10.1093/nar/gks808
590 Limbo, S., Torri, L., Sinelli, N., Franzetti, L., & Casiraghi, E. (2010). Evaluation and predictive
591 modeling of shelf life of minced beef stored in high-oxygen modified atmosphere packaging at
592 different temperatures. *Meat Science*, *84*(1), 129–136.
593 https://doi.org/10.1016/J.MEATSCI.2009.08.035
594 Luo, W., Friedman, M. S., Shedden, K., Hankenson, K. D., & Woolf, P. J. (2009). GAGE: Generally
595 applicable gene set enrichment for pathway analysis. *BMC Bioinformatics*, *10*, 1–17.
596 https://doi.org/10.1186/1471-2105-10-161

597 Luong, N. D. M., Coroller, L., Zagorec, M., Membré, J. M., & Guillou, S. (2020). Spoilage of chilled
598 fresh meat products during storage: A quantitative analysis of literature data. *Microorganisms*,
599 *8*(8), 1–29. https://doi.org/10.3390/microorganisms8081198
600 Magnúsdóttir, S., Heinken, A., Kutt, L., Ravcheev, D. A., Bauer, E., Noronha, A., … Thiele, I. (2017).
601 Generation of genome-scale metabolic reconstructions for 773 members of the human gut
602 microbiota. *Nature Biotechnology*, *35*(1), 81–89. https://doi.org/10.1038/nbt.3703
603 McMurdie, P. J., & Holmes, S. (2013). Phyloseq: An R Package for Reproducible Interactive Analysis
604 and Graphics of Microbiome Census Data. *PLoS ONE*, *8*(4).
605 https://doi.org/10.1371/journal.pone.0061217
606 Mentana, A., Conte, A., Del Nobile, M. A., Quinto, M., & Centonze, D. (2019). Volatile organic
607 compound data of ready-to-cook tuna fish-burgers: Time evolution in function of different and/or
608 combined mild preservation technologies and relevant statistical analysis. *Data in Brief*, *25*,
609 104371. https://doi.org/10.1016/j.dib.2019.104371
610 Mikami, N., Toyotome, T., Yamashiro, Y., Sugo, K., Yoshitomi, K., Takaya, M., … Shimada, K.
611 (2021). Dry-aged beef manufactured in Japan: Microbiota identification and their effects on
612 product characteristics. *Food Research International*, *140*(December 2020), 110020.
613 https://doi.org/10.1016/j.foodres.2020.110020
614 Mota-Gutierrez, J., Ferrocino, I., Rantsiou, K., & Cocolin, L. (2019). Metataxonomic comparison
615 between internal transcribed spacer and 26S ribosomal large subunit (LSU) rDNA gene.
616 *International Journal of Food Microbiology*, *290*(July 2018), 132–140.
617 https://doi.org/10.1016/j.ijfoodmicro.2018.10.010
618 Oh, H., Lee, H. J., Lee, J., Jo, C., & Yoon, Y. (2019). Identification of Microorganisms Associated
619 with the Quality Improvement of Dry-Aged Beef Through Microbiome Analysis and DNA
620 Sequencing, and Evaluation of Their Effects on Beef Quality. *Journal of Food Science*, *84*(10),

2944–2954. https://doi.org/10.1111/1750-3841.14813

Patumcharoenpol, P., Nakphaichit, M., Panagiotou, G., Senavonge, A., Suratannon, N., & Vongsangnak, W. (2021). MetGEMs Toolbox: Metagenome-scale models as integrative toolbox for uncovering metabolic functions and routes of human gut microbiome. *PLoS Computational Biology*, *17*(1 December), 1–18. https://doi.org/10.1371/journal.pcbi.1008487

Pennacchia, C., Ercolini, D., & Villani, F. (2011). Spoilage-related microbiota associated with chilled beef stored in air or vacuum pack. *Food Microbiology*, *28*(1), 84–93. https://doi.org/10.1016/j.fm.2010.08.010

Pieszczek, L., Czarnik-Matusewicz, H., & Daszykowski, M. (2018). Identification of ground meat species using near-infrared spectroscopy and class modeling techniques – Aspects of optimization and validation using a one-class classification model. *Meat Science*, *139*(January), 15–24. https://doi.org/10.1016/j.meatsci.2018.01.009

Pothakos, V., Devlieghere, F., Villani, F., Björkroth, J., & Ercolini, D. (2015). Lactic acid bacteria and their controversial role in fresh meat spoilage. *Meat Science*, *109*, 66–74. https://doi.org/10.1016/j.meatsci.2015.04.014

Pothakos, V., Snauwaert, C., De Vos, P., Huys, G., & Devlieghere, F. (2014). Psychrotrophic members of Leuconostoc gasicomitatum, Leuconostoc gelidum and Lactococcus piscium dominate at the end of shelf-life in packaged and chilled-stored food products in Belgium. *Food Microbiology*, *39*, 61–67. https://doi.org/10.1016/j.fm.2013.11.005

Price, M. N., Dehal, P. S., & Arkin, A. P. (2009). Fasttree: Computing large minimum evolution trees with profiles instead of a distance matrix. *Molecular Biology and Evolution*, *26*(7), 1641–1650. https://doi.org/10.1093/molbev/msp077

Rahkila, R., Nieminen, T., Johansson, P., Säde, E., & Björkroth, J. (2012). Characterization and evaluation of the spoilage potential of Lactococcus piscium isolates from modified atmosphere

packaged meat. *International Journal of Food Microbiology*, *156*(1), 50–59. https://doi.org/10.1016/j.ijfoodmicro.2012.02.022

Redondo-Solano, M., Guzmán-Saborío, P., Ramírez-Chavarría, F., Chaves-Ulate, C., Araya-Quesada, Y., & Araya-Morice, A. (2021). Effect of the type of packaging on the shelf life of ground rabbit meat. *Food Science and Technology International*, 1–10. https://doi.org/10.1177/10820132211003705

Rhoads, A., & Au, K. F. (2015). PacBio Sequencing and Its Applications. *Genomics, Proteomics and Bioinformatics*, *13*(5), 278–289. https://doi.org/10.1016/j.gpb.2015.08.002

Ryu, S., Park, M. R., Maburutse, B. E., Lee, W. J., Park, D. J., Cho, S., … Kim, Y. (2018). Diversity and characteristics of the meat microbiological community on dry aged beef. *Journal of Microbiology and Biotechnology*, *28*(1), 105–108. https://doi.org/10.4014/jmb.1708.08065

Sade, E., Penttinen, K., Björkroth, J., & Hultman, J. (2017). Exploring lot-to-lot variation in spoilage bacterial communities on commercial modified atmosphere packaged beef. *Food Microbiology*, *62*, 147–152. https://doi.org/10.1016/j.fm.2016.10.004

Stellato, G., Storia, A. La, Filippis, F. De, Borriello, G., Villani, F., & Ercolini, D. (2016). Overlap of spoilage microbiota between meat and meat processing environment in small-scale and large-scale retail distribution. *Applied and Environmental Microbiology*, *82*(April), 4045–4054. https://doi.org/10.1128/AEM.00793-16

Stoops, J., Ruyters, S., Busschaert, P., Spaepen, R., Verreth, C., Claes, J., … Van Campenhout, L. (2015). Bacterial community dynamics during cold storage of minced meat packaged under modified atmosphere and supplemented with different preservatives. *Food Microbiology*, *48*, 192–199. https://doi.org/10.1016/j.fm.2014.12.012

Torondel, B., Ensink, J. H. J., Gundogdu, O., Ijaz, U. Z., Parkhill, J., Abdelahi, F., … Quince, C. (2016). Assessment of the influence of intrinsic environmental and geographical factors on the

669 bacterial ecology of pit latrines. *Microbial Biotechnology*, *9*(2), 209–223.
670 https://doi.org/10.1111/1751-7915.12334
671 Valerio, F., Skandamis, P. N., Failla, S., Contò, M., Biase, M. Di, Bavaro, A. R., … Lavermicocca, P.
672 (2020). Microbiological and physicochemical parameters for predicting quality of fat and low-fat
673 raw ground beef during refrigerated aerobic storage. *Journal of Food Science*, *85*(2), 465–476.
674 https://doi.org/10.1111/1750-3841.15000
675 van Dijk, E. L., Jaszczyszyn, Y., Naquin, D., & Thermes, C. (2018). The Third Revolution in
676 Sequencing Technology. *Trends in Genetics*, *34*(9), 666–681.
677 https://doi.org/10.1016/j.tig.2018.05.008
678 Wang, Q., Garrity, G. M., Tiedje, J. M., & Cole, J. R. (2007). Naive Bayesian classifier for rapid
679 assignment of rRNA sequences into the new bacterial taxonomy. *Applied and Environmental*
680 *Microbiology*, *73*(16), 5261–5267. https://doi.org/10.1128/AEM.00062-07
681 Yang, C., Che, Y., Qi, Y., Liang, P., & Song, C. (2017). High-Throughput Sequencing of Viable
682 Microbial Communities in Raw Pork Subjected to a Fast Cooling Process. *Journal of Food*
683 *Science*, *82*(1), 145–153. https://doi.org/10.1111/1750-3841.13566
684 Zhang, D., Wang, Y., Shen, S., Hou, Y., Chen, Y., & Wang, T. (2020). The mycobiota of the human
685 body: a spark can start a prairie fire. *Gut Microbes*, *11*(4), 655–679.
686 https://doi.org/10.1080/19490976.2020.1731287
687
688
689
690
691
692

693 **Tables and figures legends**

694

695 **Fig. 1. Microbiological dynamics during hamburgers vacuum storage at 4 °C.** Charts showing the
696 viable counts (mean ± SD) of: Coagulase Negative Cocci (CNC); *Enterobacteriaceae*; Lactic Acid
697 Bacteria (LAB); Total Mesophilic Bacterial counts (TVC) and yeasts. Dashed line indicates the shelf-
698 life end (14^{th} day).

699

700 **Fig. 2. Principal Component Analysis (PCA) of the fifty-two VOCs detected in the hamburgers.**
701 Score plots highlighting distribution of the samples in relation to the time (**A**) and batch (**B**); significant
702 separation between samples is reported (Anosim and ADONIS tests). Loading plot (**C**) and contribution
703 (**D**) of each variable (VOCs) on the variance explained by the first two components (Dim1, Dim2) of the
704 PCA.

705

706 **Fig. 3. Composition of bacterial community during hamburgers vacuum storage.** Stacked bar plots
707 **(A)** showing microbiota composition (relative abundance) at the highest taxonomic level assigned
708 (asterisks highlight 100 % of ASVs similarity to reference taxa) and relative colour coding key. Samples
709 are grouped by batch and sequentially displayed according to the time; taxa are sorted in the legend from
710 the most to the least abundant (> 0.5 %). Box plots **(B)** displaying Log-transformed abundances of the
711 core species/genera in the two batches along three distinct storage phases: production, shelf-life and
712 expired. Points display each single observation and are coloured according to belonging batch. Asterisks
713 are highlighting significant differences (Wilcoxon's test) between batches at each phase (*P*-value [FDR
714 adjusted]: *= <0.05; **= <0.01, ***= <0.001); differences among phases within each batch are shown
715 by connectors and *P*-value (Kruskal-Wallis and Pairwise Wilcoxon tests [FDR adjusted). PCoA charts
716 **(C)** displaying for each batch the weighted UniFrac distance matrix (β-diversity). Days and phases of

storage are defined by different colours and shapes (legend); dashed ellipses are indicating significant different communities (P <0.001 [FDR adjusted], ANOSIM and Adonis tests).

Figure 3. Composition of fungal community during hamburgers vacuum storage. Stacked bar plots showing mycobiota composition (relative abundance) at the highest taxonomic level assigned and relative colour coding key. Samples are grouped by batch and sequentially displayed according to the time; taxa are sorted in the legend from the most to the least abundant (> 1 %).

Fig. 5. Co-occurrence/exclusion network of the hamburger microbiota and mycobiota. Network is constructed with bacterial and fungal ASVs (nodes), which are pairwise connected by lines (edges) in relation to significant SparCC correlation (100 bootstraps; pseudo *P-value* < 0.001). Nodes are made proportional to ASVs occurrences and coloured in relation to the belonging kingdom in **A** and co-occurring modules in **B**, respectively, as reported in the relative colour coding keys. Network modularity was calculated considering only co-occurrences by means of the community detection algorithm implemented in Gephi 0.9.2-beta (https://gephi.org). Edges thicknesses are made proportional to SparCC correlation value and colours indicate negative (red; SparCC correlation < -0.5) or positive (green; SparCC correlation > 0.5) correlations; lengths have no specific meaning. In the graph **B,** only positive correlations are shown. In the stacked-area plots (**C**) the cumulative relative abundances of each module is displayed along the time (average of the three replicates) for each batch and considering separately fungal and bacterial ASVs. Detailed information on correlation types are reported in **Supplementary Table 3**.

741

742

743 **Fig. 6. Biplot of the Non-Multidimensional Scaling (NMDS) analysis with best fitting VOCs and**
744 **taxa.** NMDS of the samples based on bacterial species composition with the set of VOCs (grey arrows)
745 and taxa (blue arrows) that are significantly correlated (Pearson; $P < 0.001$) with the NDMS distribution.
746 Arrows indicate the direction of change of each variable (VOCs and taxa). Only the main species were
747 considered for NMDS (> 0.5 % of average abundances); dots (samples) are shaped and coloured in
748 relation to three temporal phases and batches (legend).

749

Supplementary Tables:

Supplementary Table 1. The fifty-two VOCs detected in the headspace of vacuum packaged hamburger during the thirty days of storage at 4 °C. Data are the means of three replicates (n=3; ± std error mean) and reported as µg/g. Asterisk are highlighting significant differences between batches at each day of sampling (T-test), *P*-value: *=< 0.05, **=< 0.01, ***=< 0.001. Different letters indicate significant differences (ANOVA and Tukey's post hoc tests; *P*-value < 0.05) between sampling days (0, 4, 8, 15, 30) in the batch A (a, b, c) and B (x, y, z), respectively.

Supplementary Table 2. Variance in biological dissimilarity explained by each categorical variable (batch, time, or their interactions) in the core bacterial and fungal communities. Variance explained (R^2) and statistical significance (*P*-value) quantified by Permutational Analysis of Variance (PERMANOVA) test with Bray–Curtis dissimilarity.

Supplementary Table 3. Summary of positive and negative SparCC correlations detected among bacterial and fungal ASVs.

Supplementary Table 4. Correlation coefficients (Pearson's moment correlation) of l variables (VOCs and taxa) with NMDS ordination.

Supplementary Figures:

Supplementary Figure 1. Box plots displaying Log-transformed abundances and alpha-diversity metrics significantly different (Wilcoxon's test; *P*-value [FDR adjusted]: <0.05) between batch A and B (all sampling points considered together).

Supplementary Figure 2. Correlation between metataxonomic and volatilomic data. Tile plots showing existing correlation between VOCs and ASVs merged at the species/genus level. Colours represents level of Spearman's Rho correlation (from -1 to 1; caption) and significant positive and negative correlations are highlighted with asterisks (FDR: *= P <0.05; **= P <0.01; ***= P <0.001).

Supplementary Figure 3. Metabolic pathways differentially represented in the two batches on the base of inferred bacterial metagenomes**;** box plots show the results of pathways enrichment analysis (*gage* Bioconductor) with all metabolic pathways significantly (*gage* enrichment statistic: $P < 0.001$) overrepresented in batch A and B.

Fig. 1

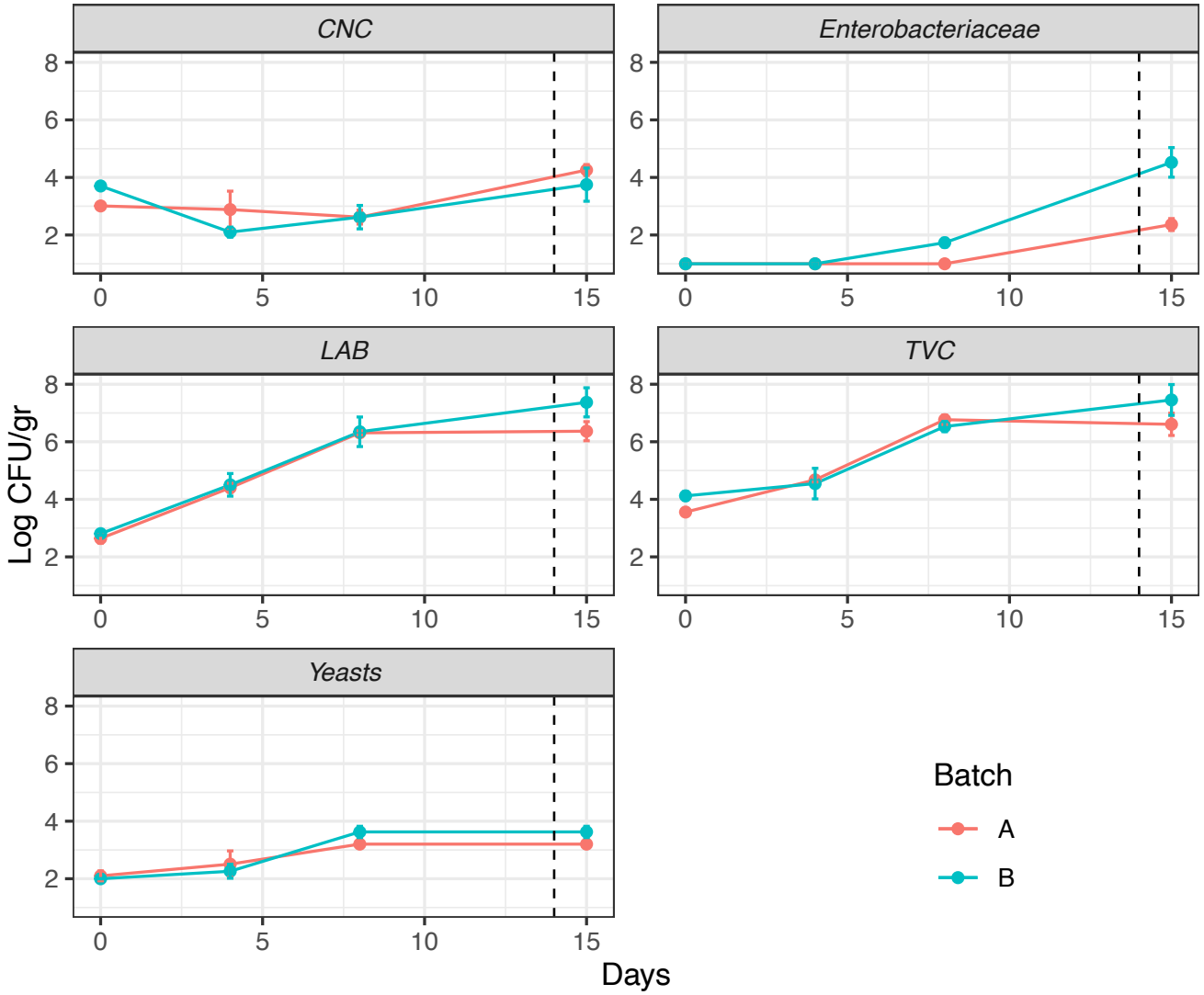
CNC
Enterobacteriaceae
LAB
TVC
Yeasts
Log CFU/gr
Days
Batch
A
B

Fig. 2.

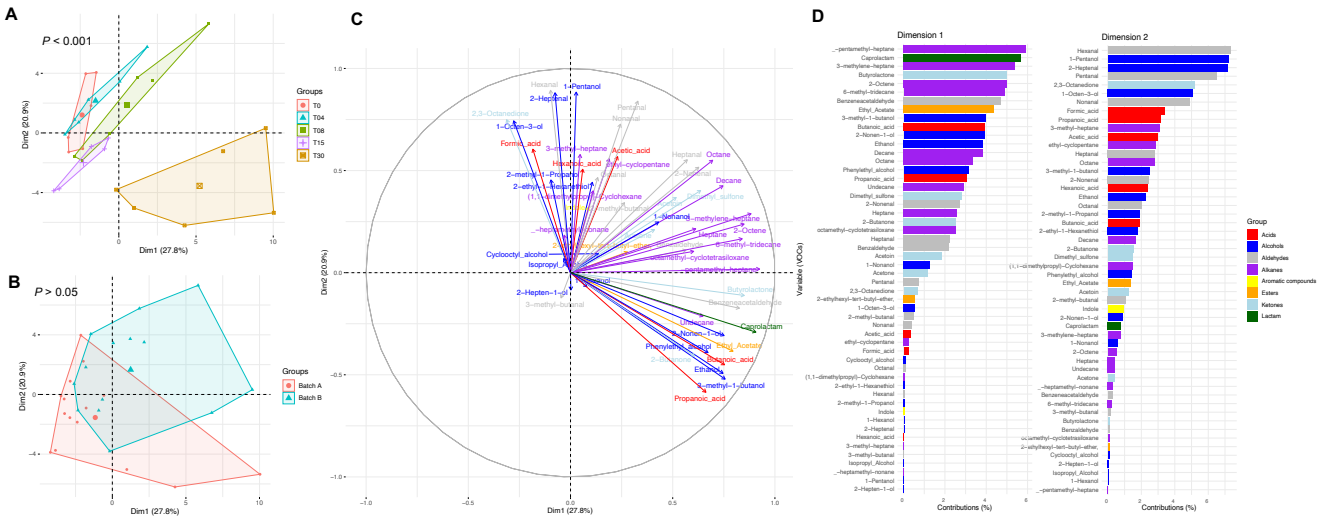
A
P < 0.001
Dim2 (20.9%)
Dim1 (27.8%)
Groups
T0
T04
T08
T15
T30
B
P > 0.05
Dim2 (20.9%)
Dim1 (27.8%)
Groups
Batch A
Batch B
C
Dim2 (20.9%)
Dim1 (27.8%)
Variable (VOCs)
1-Pentanol
2-Heptanal
1-Octen-3-ol
Formic_acid
3-methyl-heptane
Acetic_acid
Hexanoic_acid
Octyl-cyclopentane
2-methyl-1-Propanol
2-ethyl-1-Hexanethiol
Cyclohexane
1-Nonanol
Cyclooctyl_alcohol
Isopropyl_Alcohol
2-Hepten-1-ol
3-methyl-butanol
Hexanal
Pentanal
Nonanal
2,3-Octanedione
Heptanal
Octanal
Decane
Dimethyl_sulfone
3-methylene-heptane
Heptane
2-Octene
6-methyl-tridecane
Octamethyl-cyclotetrasiloxane
Butyrolactone
Benzeneacetaldehyde
Caprolactam
Undecane
2-Nonen-1-ol
Phenylethyl_alcohol
Ethyl_Acetate
Butanoic_acid
Ethanol
3-methyl-1-butanol
Propanoic_acid
D
Dimension 1
Dimension 2
Contributions (%)
Contributions (%)
Group
Acids
Alcohols
Aldehydes
Alkanes
Aromatic compounds
Esters
Ketones
Lactam

Fig. 3

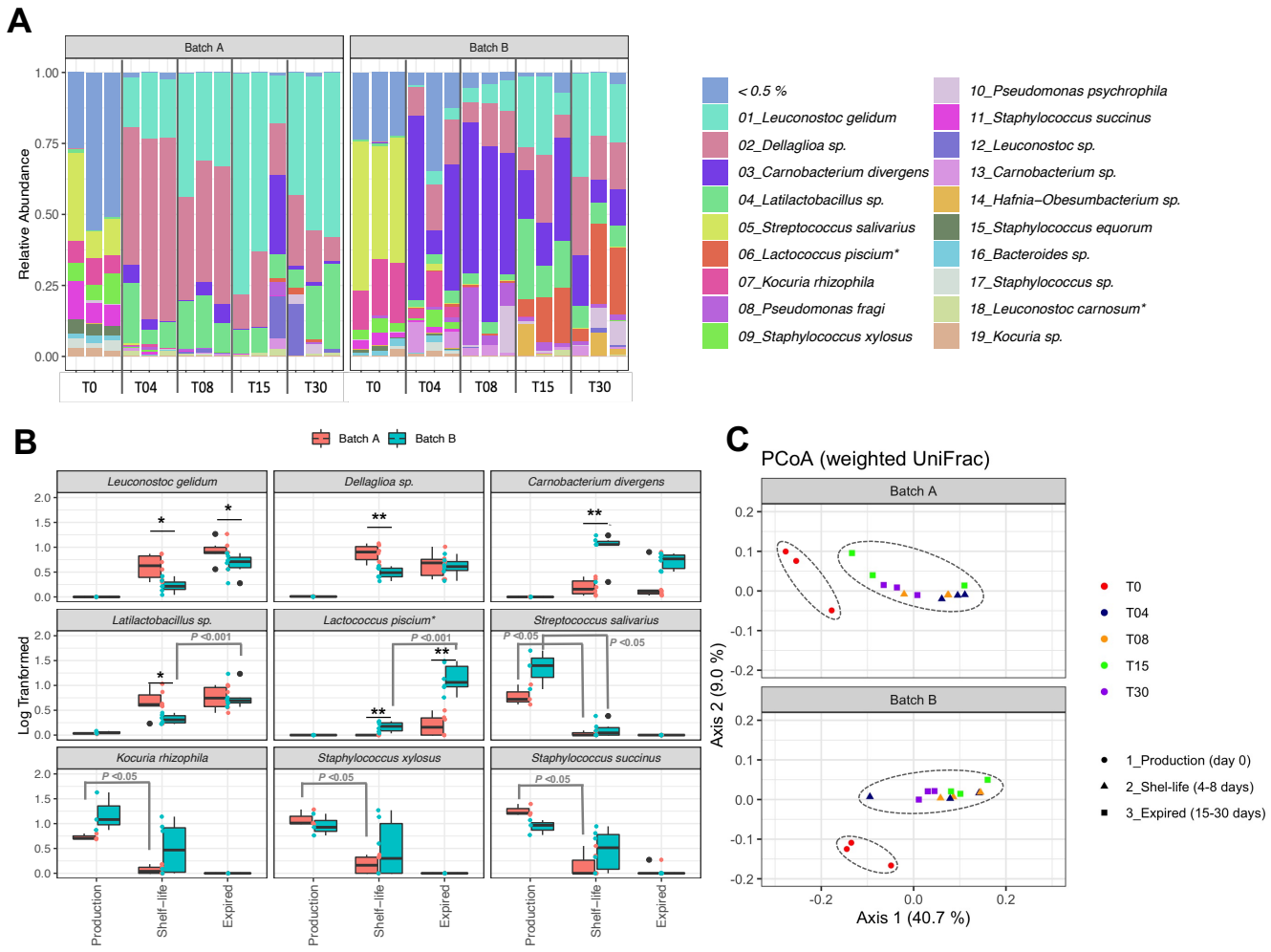

818

819 **Fig. 4**

820

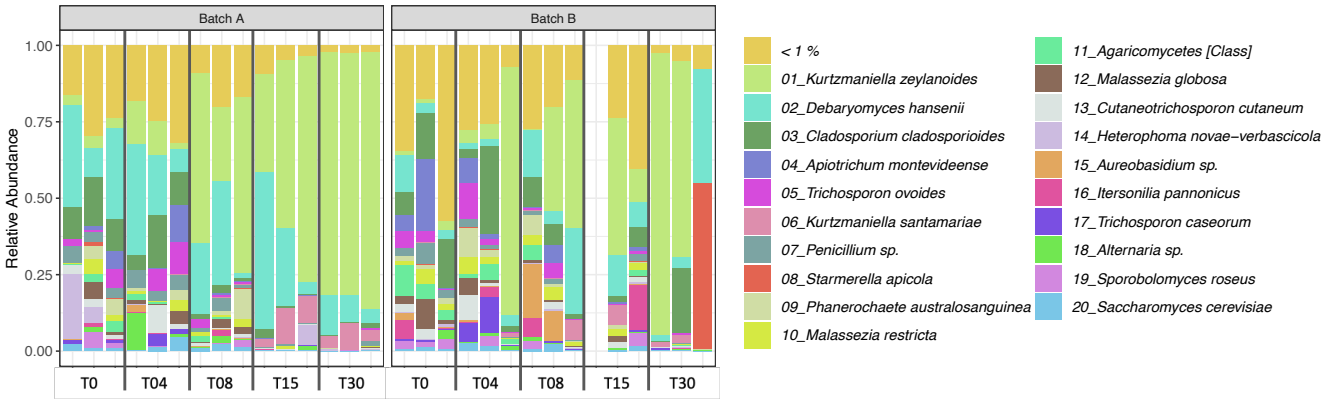

821

822

823 **Fig. 5**

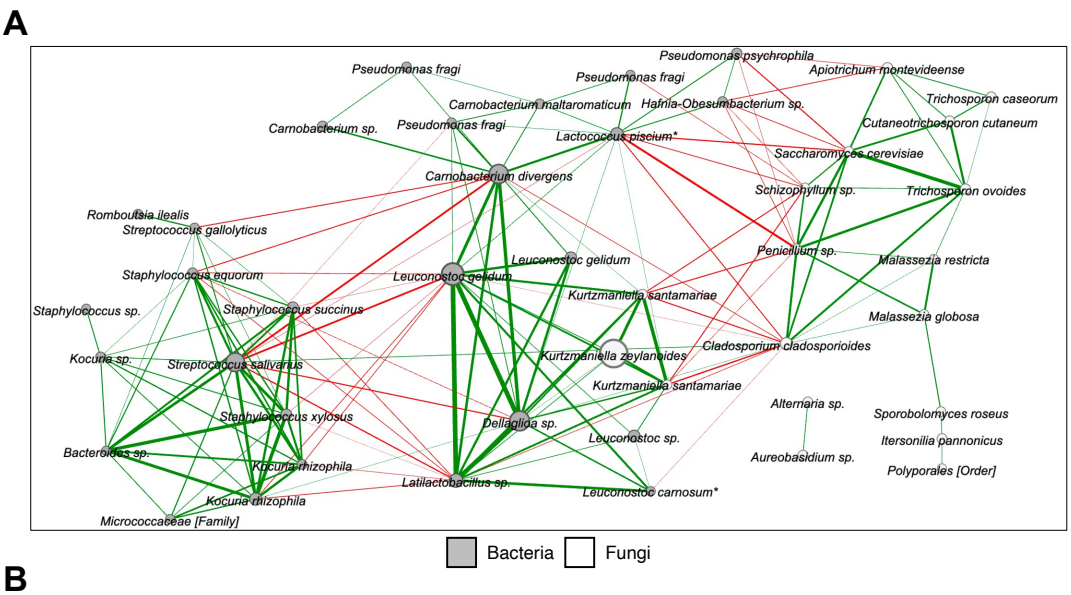
A
Pseudomonas psychrophila
Pseudomonas fragi
Pseudomonas fragi
Apiotrichum montevideense
Trichosporon caseorum
Carnobacterium maltaromaticum
Hafnia-Obesumbacterium sp.
Carnobacterium sp.
Pseudomonas fragi
Lactococcus piscium*
Cutaneotrichosporon cutaneum
Saccharomyces cerevisiae
Carnobacterium divergens
Schizophyllum sp.
Trichosporon ovoides
Romboutsia ilealis
Streptococcus gallolyticus
Penicillium sp.
Malassezia restricta
Leuconostoc gelidum
Staphylococcus equorum
Leuconostoc gelidum
Kurtzmaniella santamariae
Staphylococcus sp.
Staphylococcus succinus
Malassezia globosa
Kocuria sp.
Streptococcus salivarius
Kurtzmaniella zeylanoides
Cladosporium cladosporioides
Kurtzmaniella santamariae
Alternaria sp.
Staphylococcus xylosus
Sporobolomyces roseus
Dellaglioa sp.
Leuconostoc sp.
Itersonilia pannonicus
Bacteroides sp.
Aureobasidium sp.
Kocuria rhizophila
Polyporales [Order]
Latilactobacillus sp.
Leuconostoc carnosum*
Kocuria rhizophila
Micrococcaceae [Family]
Bacteria
Fungi
B
Pseudomonas psychrophila
Pseudomonas fragi
Pseudomonas fragi
Apiotrichum montevideense
Trichosporon caseorum
Carnobacterium maltaromaticum
Hafnia-Obesumbacterium sp.
Carnobacterium sp.
Pseudomonas fragi
Lactococcus piscium*
Cutaneotrichosporon cutaneum
Saccharomyces cerevisiae
Carnobacterium divergens
Schizophyllum sp.
Trichosporon ovoides
Romboutsia ilealis
Streptococcus gallolyticus
Penicillium sp.
Malassezia restricta
Leuconostoc gelidum
Staphylococcus equorum
Leuconostoc gelidum
Kurtzmaniella santamariae
Staphylococcus sp.
Staphylococcus succinus
Malassezia globosa
Kocuria sp.
Streptococcus salivarius
Kurtzmaniella zeylanoides
Cladosporium cladosporioides
Kurtzmaniella santamariae
Alternaria sp.
Staphylococcus xylosus
Sporobolomyces roseus
Dellaglioa sp.
Leuconostoc sp.
Itersonilia pannonicus
Bacteroides sp.
Aureobasidium sp.
Kocuria rhizophila
Polyporales [Order]
Latilactobacillus sp.
Leuconostoc carnosum*
Kocuria rhizophila
Micrococcaceae [Family]
C
Module 0
Module 1
Module 2
Module 3
Module 4
Module 5
Batch A
Batch B
Relative Abundance (average)
Bacteria
Fungi
1.00
0.75
0.50
0.25
0.00
0
10
20
30
Days

824

825

826 **Fig. 6**

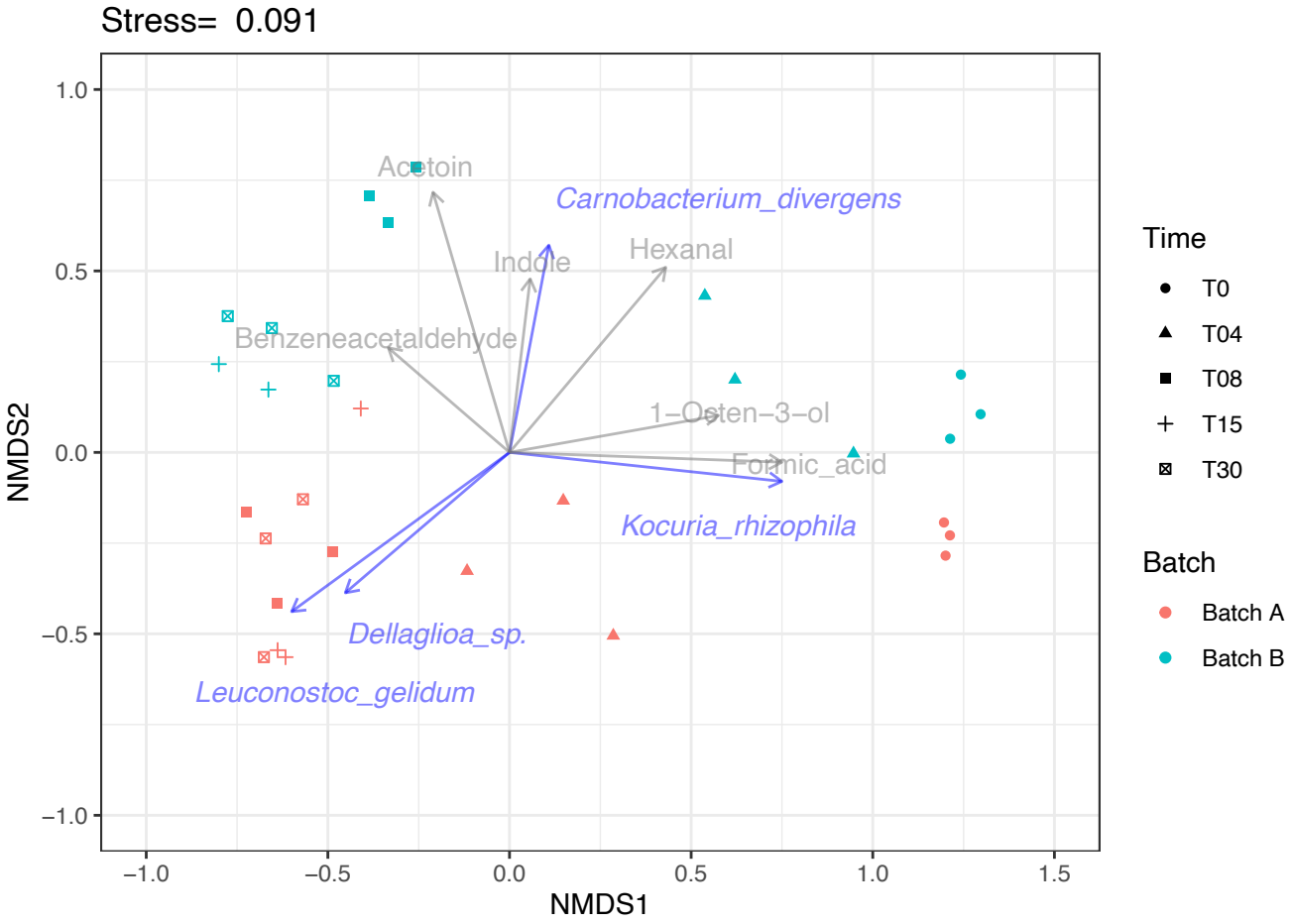

827

828

829

830

831

832

833

834

835

836

837

S Figure 1

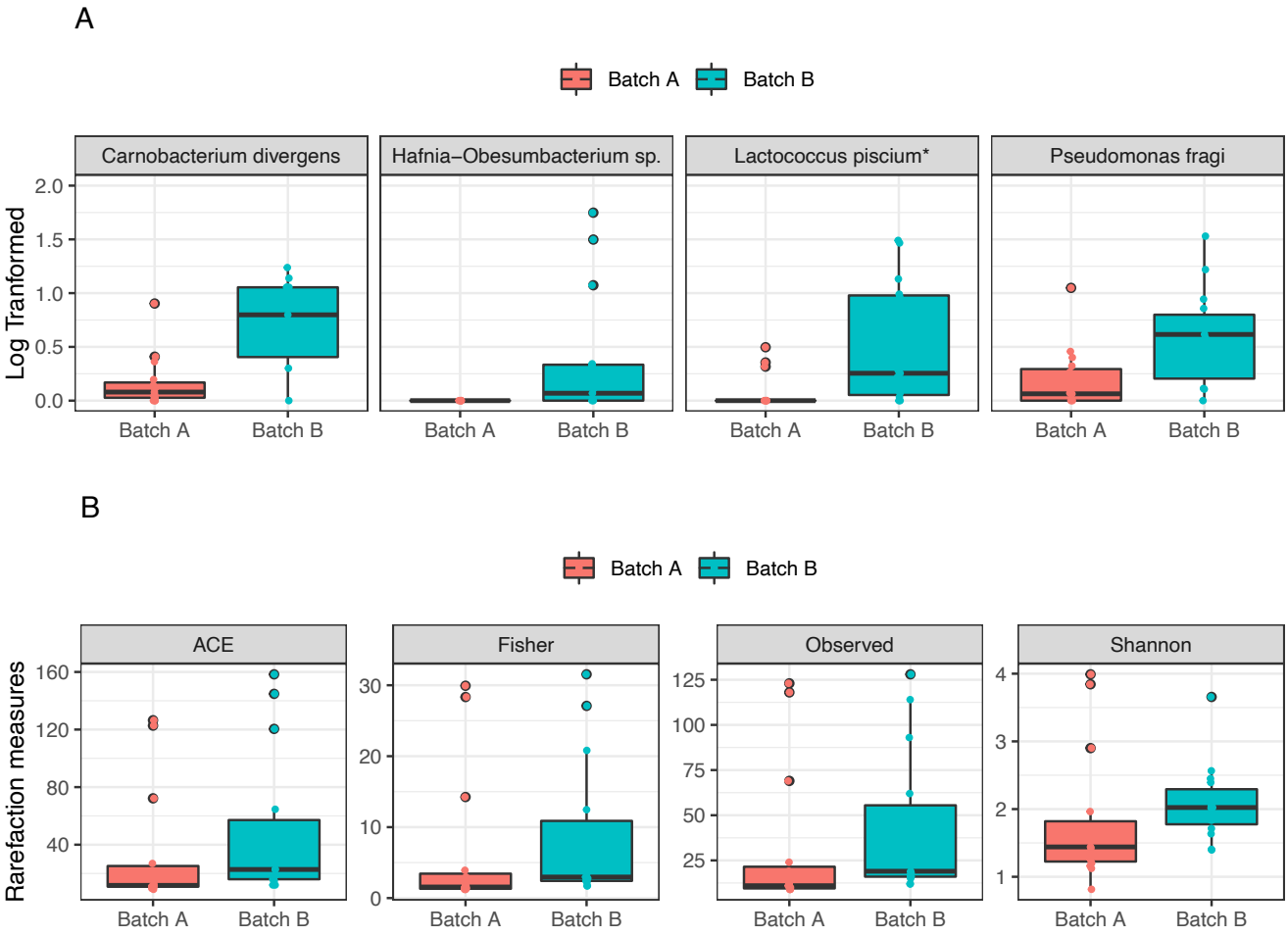
A
Batch A
Batch B
Carnobacterium divergens
Hafnia−Obesumbacterium sp.
Lactococcus piscium*
Pseudomonas fragi
Log Tranformed
2.0
1.5
1.0
0.5
0.0
Batch A
Batch B
B
Batch A
Batch B
ACE
Fisher
Observed
Shannon
Rarefaction measures
160
120
80
40
30
20
10
0
125
100
75
50
25
4
3
2
1
Batch A
Batch B

S Figure 2

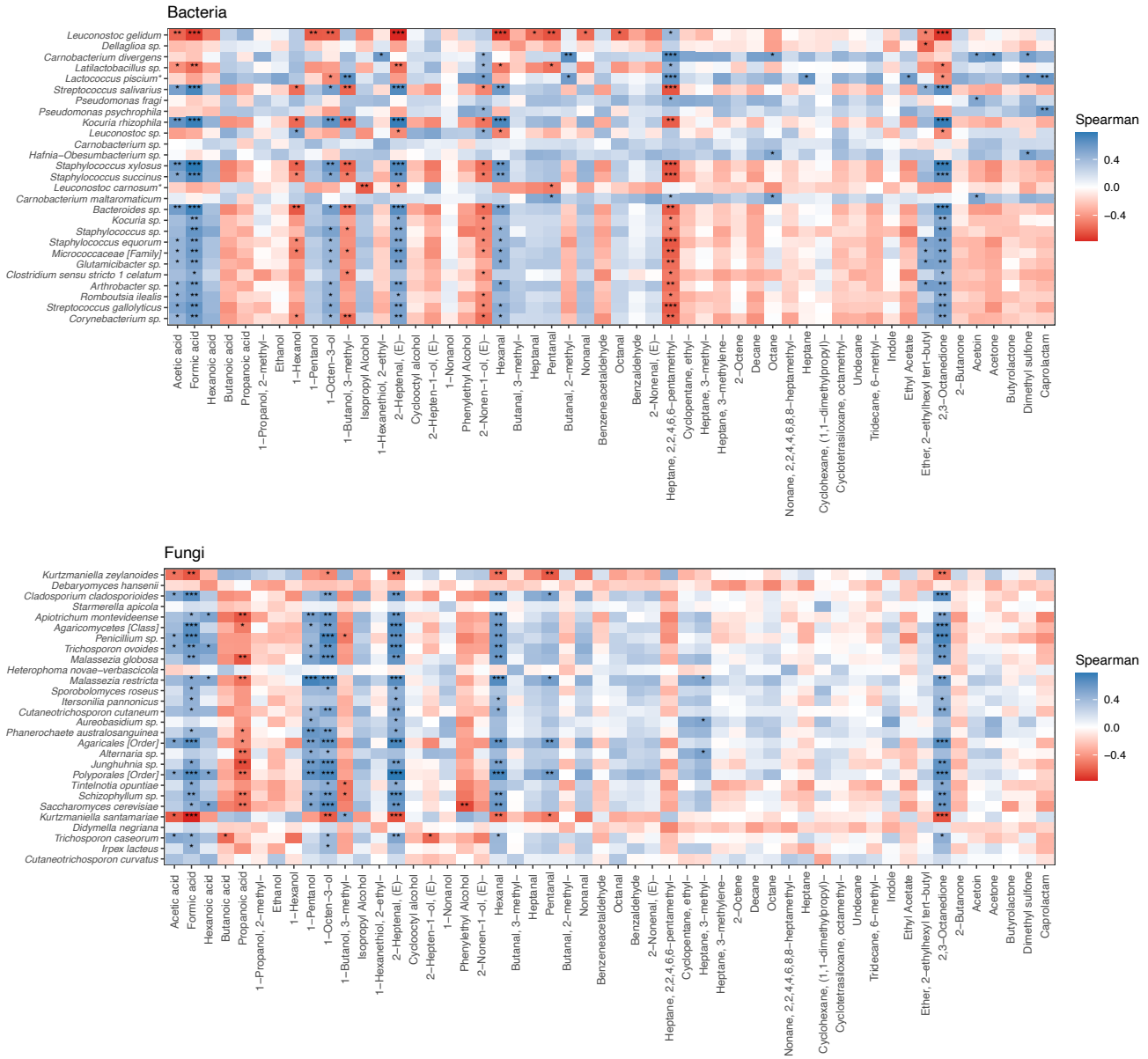
Bacteria
Leuconostoc gelidum
Dellaglioa sp.
Carnobacterium divergens
Latilactobacillus sp.
Lactococcus piscium*
Streptococcus salivarius
Pseudomonas fragi
Pseudomonas psychrophila
Kocuria rhizophila
Leuconostoc sp.
Carnobacterium sp.
Hafnia−Obesumbacterium sp.
Staphylococcus xylosus
Staphylococcus succinus
Leuconostoc carnosum*
Carnobacterium maltaromaticum
Bacteroides sp.
Kocuria sp.
Staphylococcus sp.
Staphylococcus equorum
Micrococcaceae [Family]
Glutamicibacter sp.
Clostridium sensu stricto 1 celatum
Arthrobacter sp.
Romboutsia ilealis
Streptococcus gallolyticus
Corynebacterium sp.
Acetic acid
Formic acid
Hexanoic acid
Butanoic acid
Propanoic acid
1−Propanol, 2−methyl−
Ethanol
1−Hexanol
1−Pentanol
1−Octen−3−ol
1−Butanol, 3−methyl−
Isopropyl Alcohol
1−Hexanethiol, 2−ethyl−
2−Heptenal, (E)−
Cyclooctyl alcohol
2−Hepten−1−ol, (E)−
1−Nonanol
Phenylethyl Alcohol
2−Nonen−1−ol, (E)−
Hexanal
Butanal, 3−methyl−
Heptanal
Pentanal
Butanal, 2−methyl−
Nonanal
Benzeneacetaldehyde
Octanal
Benzaldehyde
2−Nonenal, (E)−
Heptane, 2,2,4,6,6−pentamethyl−
Cyclopentane, ethyl−
Heptane, 3−methyl−
Heptane, 3−methylene−
2−Octene
Decane
Octane
Nonane, 2,2,4,4,6,8,8−heptamethyl−
Heptane
Cyclohexane, (1,1−dimethylpropyl)−
Cyclotetrasiloxane, octamethyl−
Undecane
Tridecane, 6−methyl−
Indole
Ethyl Acetate
Ether, 2−ethylhexyl tert−butyl
2,3−Octanedione
2−Butanone
Acetoin
Acetone
Butyrolactone
Dimethyl sulfone
Caprolactam
Spearman
0.4
0.0
−0.4
Fungi
Kurtzmaniella zeylanoides
Debaryomyces hansenii
Cladosporium cladosporioides
Starmerella apicola
Apiotrichum montevideense
Agaricomycetes [Class]
Penicillium sp.
Trichosporon ovoides
Malassezia globosa
Heterophoma novae−verbascicola
Malassezia restricta
Sporobolomyces roseus
Itersonilia pannonicus
Cutaneotrichosporon cutaneum
Aureobasidium sp.
Phanerochaete australosanguinea
Agaricales [Order]
Alternaria sp.
Junghuhnia sp.
Polyporales [Order]
Tintelnotia opuntiae
Schizophyllum sp.
Saccharomyces cerevisiae
Kurtzmaniella santamariae
Didymella negriana
Trichosporon caseorum
Irpex lacteus
Cutaneotrichosporon curvatus
Spearman
0.4
0.0
−0.4

S Figure 3


Overrepresented in Batch A
Overrepresented in Batch B
Log2 Fold Abundance
AM_ko00340
Histidine metabolism
AM_ko00480
Glutathione metabolism
AM_ko01230
Biosynthesis of amino acids
CM_ko00010
Glycolysis/Gluconeogenesis
CM_ko00040
Pentose/glucuronate interconversions
CM_ko00051
Fructose/mannose metabolism
CM_ko00052
Galactose metabolism
CM_ko00500
Starch/sucrose metabolism
LM_ko00564
Glycerophospholipid metabolism
AM_ko00280
Valine/leucine/isoleucine degradation
AM_ko00410
beta−Alanine metabolism
CM_ko00020
Citrate cycle (TCA cycle)
CM_ko00630
Glyoxylate/dicarboxylate metabolism
CM_ko00640
Propanoate metabolism
CM_ko00650
Butanoate metabolism
GBM_ko00540
Lipopolysaccharide biosynthesis
A
B
AM: Aminoacid metabolism
CM: Carbohydrate metabolism
LM: Lipid metabolism
GBM: Glycan biosynthesis and metabolism
Batch A
Batch B